

Mass Dependence of Disappearance of Transverse Flow

Aman D. Sood and Rajeev K. Puri

Physics Department, Panjab University, Chandigarh -160 014, India

A complete theoretical study is presented for the disappearance of flow, for the first time, by analyzing 15 reactions with masses between 47 and 476 units. We demonstrate that the effect of nucleon-nucleon cross-section reduces to insignificant level for heavier colliding nuclei in agreement with previous studies. A stiff equation of state with nucleon-nucleon cross-sections $\sigma=35\text{-}40$ mb is able to explain all the measured balance energies within few percent. A power law ($\propto A^\tau$) is also given for the mass dependence of the disappearance of flow which is in excellent agreement with experimental data.

PACS numbers:

I. INTRODUCTION

The heavy-ion collisions at intermediate energies provide a rich physical insight into the reaction dynamics. One has measured (and/or predicted) several new phenomena that may shed light on the nature of hot and dense nuclear matter formed during a collision. In addition, one also hopes to understand the nature of nuclear interactions in medium. The prediction of collective transverse flow by the hydrodynamical model was a very important step towards the understanding of excited nuclear matter [1]. The collective transverse flow was found to be very sensitive towards different signals of excited nuclear matter. Apart from the transverse flow, one has also proposed e.g. differential flow [2], and elliptic flow [3]. All these quantities are assumed to be sensitive towards the (nuclear matter) equation of state and/or nucleon-nucleon (nn) cross-section \Rightarrow *the ultimate goal of the intermediate energy heavy-ion collisions*. One should however, keep in the mind that the reaction dynamics depends also on the incident energy as well as on the impact parameter of the reaction. At low incident energies, the dynamics is governed by the attractive mean field whereas the repulsive interactions decide the fate of a reaction at higher incident energies. Naturally, the effect of nn collisions decreases with decrease in the incident energy. The dominance of the attractive mean field (at low incident energies) may prompt the emission of particles into backward hemisphere whereas if nn scatterings dominate, the particle emission is likely to be in the forward hemisphere. Therefore, while going from the low incident energy to higher energy, the attractive interactions may be balanced by the repulsive interactions, resulting in the net zero flow (i.e. the disappearance of flow). The energy at which the flow disappears is termed as the balance energy [4].

During the last few years, extensive efforts have been made to measure and understand the disappearance of flow [5, 6, 7, 8, 9, 10, 11, 12, 13, 14, 15, 16, 17]. One has measured the balance energy (E_{bal}) in $^{12}\text{C}+^{12}\text{C}$ [5], $^{20}\text{Ne}+^{27}\text{Al}$ [5], $^{36}\text{Ar}+^{27}\text{Al}$ [7, 17], $^{40}\text{Ar}+^{27}\text{Al}$ [8], $^{40}\text{Ar}+^{45}\text{Sc}$ [5, 6, 12], $^{40}\text{Ar}+^{51}\text{V}$ [9], $^{64}\text{Zn}+^{27}\text{Al}$ [10], $^{40}\text{Ar}+^{58}\text{Ni}$ [11], $^{64}\text{Zn}+^{48}\text{Ti}$ [17], $^{58}\text{Ni}+^{58}\text{Ni}$ [11, 12, 13],

$^{58}\text{Fe}+^{58}\text{Fe}$ [13], $^{64}\text{Zn}+^{58}\text{Ni}$ [17], $^{86}\text{Kr}+^{93}\text{Nb}$ [5, 12], $^{93}\text{Nb}+^{93}\text{Nb}$ [14], $^{129}\text{Xe}+^{118}\text{Sn}$ [11], $^{139}\text{La}+^{139}\text{La}$ [14], and $^{197}\text{Au}+^{197}\text{Au}$ [12, 15, 16] systems. The very recent and accurate measurement of the balance energy E_{bal} in $^{197}\text{Au}+^{197}\text{Au}$ [12, 16] has generated a renewed interest in the field [11]. Interestingly, most of the reported reactions are symmetric in nature. It should be kept in the mind that the reaction dynamics depends also upon the asymmetry of the reaction [18]. All the above mentioned measurements were for the central collisions only. Some measurements [6, 8, 10, 11, 12, 13] however, also took the impact parameter dependence into account. As noted in ref. [12], the E_{bal} for heavier nuclei shows a little dependence on the impact parameter whereas a large variation in the E_{bal} can be seen for lighter colliding nuclei [6, 12]. The possible cause could be the fact that the disappearance of flow for heavier nuclei occurs at a much lower incident energy compared to lighter nuclei (e.g. the measured E_{bal} for $^{197}\text{Au}+^{197}\text{Au}$ is $42\pm 3\pm 1$ MeV/nucleon [16] whereas it is 111 ± 10 MeV/nucleon for $^{20}\text{Ne}+^{27}\text{Al}$ [5]). In the (nearly) absence of nn collisions at low incident energies, a little dependence should occur on impact parameter [19]. Some attempts also exist in the literature where enhancement in the E_{bal} with neutron content was found experimentally/theoretically [13, 20, 21].

The above findings reveal the measurements of balance energy in more than 15 systems ranging from very light to heavy nuclei. As a result, a power law behaviour ($\propto A^\tau$) has also been reported for E_{bal} [5, 12, 16, 17]. Earlier the power law parameter “ τ ” was supposed to be close to $-1/3$ (resulting from the interplay between the attractive mean field and repulsive nn collisions) [5] whereas the recent measurements suggest a deviation from the above mentioned power law [12, 16].

Various theoretical attempts have been made to understand the vanishing of nuclear flow. Most of these are, however, using the Boltzmann-Uehling-Uhlenbeck model [2, 3, 4, 5, 8, 10, 12, 13, 14, 16, 21, 22, 23, 24, 25, 26]. Some attempts are also reported in the literature where Quantum Molecular Dynamics (QMD) model was used [6, 20, 27, 28, 29, 30, 31]. Different theoretical attempts considered either a stiff or soft equation of state along with variety of nn cross-sections. Interestingly, out of

all these studies, only a couple of attempts exist where mass dependence of the disappearance of flow was discussed [5, 12, 16, 17, 26, 30, 31]. A careful analysis shows that in refs. [5, 26] a total mass ≤ 200 was considered for the power law studies whereas in refs. [30, 31] only heavier masses ≥ 175 were analyzed. There the E_{bal} for heavier nuclei was found to scale as approximately $1/\sqrt{A}$ [30, 31] whereas lighter and medium mass nuclei follow $A^{-1/3}$ dependence [5, 26]. Refs. [12, 16] included for the first time, a larger mass range $63/47 \leq A \leq 394$. However, even in these studies, only six systems were taken into account (note that the power law fit was made for those systems which were recorded in the 4π NSCL experiment. The data from the GANIL experiments, however, was not taken into account for fitting). The earlier mass dependence by the same group [5] also considered five systems only. We here present, for the first time, a complete study of the mass dependence in the disappearance of flow by analyzing as many as fifteen central collisions ranging from $^{20}\text{Ne}+^{27}\text{Al}$ to $^{197}\text{Au}+^{197}\text{Au}/^{238}\text{U}+^{238}\text{U}$. The corresponding experimental measurements were reported by several different groups [5, 6, 7, 8, 9, 10, 11, 12, 13, 14, 15, 16, 17]. This study, therefore, will present a unified analysis of the balance energy irrespective of the experimental setup/group. The present study is carried out within the framework of the Quantum Molecular Dynamics (QMD) model [18, 19, 20, 27, 28, 29, 30, 31, 32, 33, 34]. The details of the model are given in section 2. The results and discussion is presented in section 3 and we summarize our results in section 4.

II. THE MODEL

We describe the time evolution of a heavy-ion reaction within the framework of Quantum Molecular Dynamics (QMD) model [18, 19, 20, 27, 28, 29, 30, 31, 32, 33, 34] which is based on a molecular dynamics picture. Here each nucleon is represented by a coherent state of the form

$$\phi_\alpha(x_1, t) = \left(\frac{2}{L\pi}\right)^{\frac{3}{4}} e^{-(x_1-x_\alpha(t))^2} e^{ip_\alpha(x_1-x_\alpha)} e^{-\frac{ip_\alpha^2 t}{2m}}. \quad (1)$$

Thus, the wave function has two time dependent parameters x_α and p_α . The total n-body wave function is assumed to be a direct product of coherent states:

$$\phi = \phi_\alpha(x_1, x_\alpha, p_\alpha, t) \phi_\beta(x_2, x_\beta, p_\beta, t) \dots, \quad (2)$$

where, antisymmetrization is neglected. The initial values of the parameters are chosen in a way that the ensemble (A_T+A_P) nucleons give a proper density distribution as well as a proper momentum distribution of the projectile and target nuclei. The time evolution of the system is calculated using the generalized variational principle. We start out from the action

$$S = \int_{t_1}^{t_2} \mathcal{L}[\phi, \phi^*] d\tau, \quad (3)$$

with the Lagrange functional

$$\mathcal{L} = \left(\phi \left| i\hbar \frac{d}{dt} - H \right| \phi \right), \quad (4)$$

where the total time derivative includes the derivatives with respect to the parameters. The time evolution is obtained by the requirement that the action is stationary under the allowed variation of the wave function

$$\delta S = \delta \int_{t_1}^{t_2} \mathcal{L}[\phi, \phi^*] dt = 0. \quad (5)$$

If the true solution of the Schrödinger equation is contained in the restricted set of wave function $\phi_\alpha(x_1, x_\alpha, p_\alpha)$, this variation of the action gives the exact solution of the Schrödinger equation. If the parameter space is too restricted, we obtain that wave function in the restricted parameter space which comes close to the solution of the Schrödinger equation. Performing the variation with the test wave function (2), we obtain for each parameter λ an Euler-Lagrange equation;

$$\frac{d}{dt} \frac{\partial \mathcal{L}}{\partial \dot{\lambda}} - \frac{\partial \mathcal{L}}{\partial \lambda} = 0. \quad (6)$$

For each coherent state and a Hamiltonian of the form, $H = \sum_\alpha [T_\alpha + \frac{1}{2} \sum_{\alpha\beta} V_{\alpha\beta}]$, the Lagrangian and the Euler-Lagrange function can be easily calculated [33]

$$\mathcal{L} = \sum_\alpha \dot{\mathbf{x}}_\alpha \mathbf{p}_\alpha - \sum_\beta \langle V_{\alpha\beta} \rangle - \frac{3}{2Lm}, \quad (7)$$

$$\dot{\mathbf{x}}_\alpha = \frac{\mathbf{p}_\alpha}{m} + \nabla_{p_\alpha} \sum_\beta \langle V_{\alpha\beta} \rangle, \quad (8)$$

$$\dot{\mathbf{p}}_\alpha = -\nabla_{\mathbf{x}_\alpha} \sum_\beta \langle V_{\alpha\beta} \rangle. \quad (9)$$

Thus, the variational approach has reduced the n-body Schrödinger equation to a set of $6n$ -different equations for the parameters which can be solved numerically. If one inspects the formalism carefully, one finds that the interaction potential which is actually the Bruckner G-matrix can be divided into two parts: (i) a real part and (ii) an imaginary part. The real part of the potential acts like a potential whereas the imaginary part is proportional to the cross-section.

In the present model, interaction potential comprises of the following terms:

$$V_{\alpha\beta} = V_{loc}^2 + V_{loc}^3 + V_{Coul} + V_{Yuk}, \quad (10)$$

V_{loc} is the Skyrme force whereas V_{Coul} and V_{Yuk} define, respectively, the Coulomb and Yukawa terms. The expectation value of these potentials is calculated as

$$V_{loc}^3 = \int f_\alpha(\mathbf{p}_\alpha, \mathbf{r}_\alpha, t) f_\beta(\mathbf{p}_\beta, \mathbf{r}_\beta, t) V_I^{(2)}(\mathbf{r}_\alpha, \mathbf{r}_\beta) \times d^3\mathbf{r}_\alpha d^3\mathbf{r}_\beta d^3\mathbf{p}_\alpha d^3\mathbf{p}_\beta, \quad (11)$$

$$\begin{aligned}
V_{loc}^3 = & \int f_\alpha(\mathbf{p}_\alpha, \mathbf{r}_\alpha, t) f_\beta(\mathbf{p}_\beta, \mathbf{r}_\beta, t) f_\gamma(\mathbf{p}_\gamma, \mathbf{r}_\gamma, t) \\
& \times V_I^{(3)}(\mathbf{r}_\alpha, \mathbf{r}_\beta, \mathbf{r}_\gamma) d^3\mathbf{r}_\alpha d^3\mathbf{r}_\beta d^3\mathbf{r}_\gamma \\
& \times d^3\mathbf{p}_\alpha d^3\mathbf{p}_\beta d^3\mathbf{p}_\gamma.
\end{aligned} \tag{12}$$

Where $f_\alpha(\mathbf{p}_\alpha, \mathbf{r}_\alpha, t)$ is the Wigner density which corresponds to the wave functions (eq. 2). If we deal with the local Skyrme force only, we get

$$V^{Skyrme} = \sum_{\alpha=1}^{A_T+A_P} \left[\frac{A}{2} \sum_{\beta=1} \left(\frac{\tilde{\rho}_{\alpha\beta}}{\rho_0} \right) + \frac{B}{C+1} \sum_{\beta \neq \alpha} \left(\frac{\tilde{\rho}_{\alpha\beta}}{\rho_0} \right)^C \right]. \tag{13}$$

Here A, B and C are the Skyrme parameters which are defined according to the ground state properties of a nucleus. Different values of C lead to different equations of state. A larger value of C (=380 MeV) is often dubbed as stiff equation of state.

A number of attempts exist in the literature which study the nature of equation of state. Following refs. [2, 3, 4, 6, 8, 10, 22, 24, 26, 27, 28, 29, 30, 31], we shall also employ a stiff equation of state through out the present analysis. It should also be noted that the success rate is nearly the same for stiff and soft equations of state. Further, it has been shown in refs. [8, 10, 22, 24, 26] that the difference between E_{bal} using a stiff and soft equation of state is insignificant for central heavy-ion collisions.

The imaginary part of the potential i.e. the nn cross-section has been a point of controversy. A large number of calculations exist where a constant and isotropic cross-section is used. Following refs. [8, 10, 22, 24, 29, 30, 31, 35, 36], we also use constant energy independent cross-section. As shown by Li [25], most of the collisions below 100 MeV/nucleon happen with nn cross-section of 55 mb strength. Keeping the present energy domain into mind, the choice of a constant cross-section is justified. It has also been also shown by Zheng et al. [3] that a stiff equation of state with free nn cross-section and a soft equation of state with reduced cross-section yield nearly the same results. For comparison, we shall also use an energy dependent cross-section as fitted by Cugnon [33] (labeled as Cug) as well as a medium dependent cross-section derived from G-matrix [33] (denoted by GMC).

III. RESULTS AND DISCUSSION

Using a stiff equation of state along with different nn cross-sections, we simulated the above mentioned reactions for 1000-3000 events in each case. The reactions were followed till transverse flow saturates. The saturation time varies between 150 fm/c (for lighter colliding nuclei such as $^{20}\text{Ne}+^{27}\text{Al}$) and 300 fm/c (for heavier colliding nuclei such as $^{197}\text{Au}+^{197}\text{Au}$). In particular, we simulated $^{20}\text{Ne}+^{27}\text{Al}$ at $b=2.6103$ fm, $^{36}\text{Ar}+^{27}\text{Al}$ at $b=2$ fm, $^{40}\text{Ar}+^{27}\text{Al}$ at $b=1.6$ fm, $^{40}\text{Ar}+^{45}\text{Sc}$ at $b=3.187$ fm, $^{40}\text{Ar}+^{51}\text{V}$ at $b=2.442$ fm, $^{64}\text{Zn}+^{27}\text{Al}$ at $b=2.5$ fm, $^{40}\text{Ar}+^{58}\text{Ni}$ at $b=0-3$ fm, $^{64}\text{Zn}+^{48}\text{Ti}$ at $b=2$

fm, $^{58}\text{Ni}+^{58}\text{Ni}$ at $b=2.48$ fm, $^{64}\text{Zn}+^{58}\text{Ni}$ at $b=2$ fm, $^{86}\text{Kr}+^{93}\text{Nb}$ at $b=4.07$ fm, $^{93}\text{Nb}+^{93}\text{Nb}$ at $b=3.104$ fm, $^{129}\text{Xe}+^{Nat}\text{Sn}$ at $b=0-3$ fm, $^{139}\text{La}+^{139}\text{La}$ at $b=3.549$ fm and $^{197}\text{Au}+^{197}\text{Au}$ at $b=2.5$ fm. The choice of impact parameter is based on the experimentally extracted information [5-17]. The above reactions were simulated at incident energies between 30 MeV/nucleon and 150 MeV/nucleon depending upon the mass of the system. Naturally, a lower energy range was used for heavy nuclei whereas a higher beam energy was needed for lighter cases. The reactions were simulated at different fixed incident energies and a straight line interpolation was used to find the balance energy E_{bal} .

There are several methods used in the literature to define the nuclear transverse flow. In most of the studies, balance energy is extracted from (p_x/A) plots where one plots (p_x/A) as a function of Y_{cm}/Y_{beam} . Using a linear fit to the slope, one can define the so-called reduced flow (F). Naturally, the energy at which the reduced flow passes through zero, is called the balance energy. Alternatively, one can also use a more integrated quantity ‘‘directed transverse momentum $\langle p_x^{dir} \rangle$ ’’ which is defined as [28, 29, 30, 31, 32, 33, 34]:

$$\langle p_x^{dir} \rangle = \frac{1}{A} \sum_i \text{sign}\{Y(i)\} p_x(i), \tag{14}$$

where $Y(i)$ and $p_x(i)$ are the rapidity distribution and transverse momentum of the i th particle. In this definition, all rapidity bins are taken into account. It, therefore, presents an easier way of measuring the in-plane flow rather than complicated functions such as the (p_x/A) plots. It is worth mentioning that the balance energy is independent of the nature of emitted particle [5]. Further, the apparatus correction and acceptance does not play any role in calculating the energy of vanishing flow [5, 9].

In fig. 1, we display the final state transverse momentum $\langle p_x/A \rangle$ as a function of the rapidity which is defined as:

$$Y(i) = \frac{1}{2} \ln \frac{\mathbf{E}(i) + \mathbf{p}_z(i)}{\mathbf{E}(i) - \mathbf{p}_z(i)}, \tag{15}$$

where $\mathbf{E}(i)$ and $\mathbf{p}_z(i)$ are, respectively, the total energy and longitudinal momentum of i th particle. The upper parts are for $^{20}\text{Ne}+^{27}\text{Al}$ (at 150 fm/c) and $^{40}\text{Ar}+^{45}\text{Sc}$ (at 150 fm/c), whereas the bottom parts are for $^{139}\text{La}+^{139}\text{La}$ (at 300 fm/c) and $^{197}\text{Au}+^{197}\text{Au}$ (at 300 fm/c). The middle part is for $^{64}\text{Zn}+^{58}\text{Ni}$ (at 300 fm/c) and $^{93}\text{Nb}+^{93}\text{Nb}$ (at 300 fm/c). In all cases, the slope is negative at lower incident energies which changes to positive value at higher incident energies. Between these limits, the slope becomes almost zero at a particular energy. This zero slope energy is termed as balance energy. One also notices that a higher value of incident energy is needed in lighter cases to balance the attractive and repulsive forces. This energy decreases with increase in the mass of the system.

A look at fig. 2, where $\langle p_x^{dir} \rangle$ (instead of $\langle p_x/A \rangle$) is plotted, depicts quite similar trends. Here $\langle p_x^{dir} \rangle$ is displayed as a function of the reaction time. The $\langle p_x^{dir} \rangle$ during initial stage is always negative irrespective of the incident energy. This shows that the interactions among nuclei are attractive during the initial phase of the reaction. These interactions remain either attractive throughout the time evolution, or may turn repulsive depending on the incident energy. The transverse flow in lighter colliding nuclei saturates earlier compared to heavy colliding nuclei. One also sees a sharp transition from negative to positive flow in lighter nuclei. This transition is gradual when one analyzes the heavier nuclei. If one compares figs. 1 and 2, one finds that the disappearance of flow (where flow is zero) occurs at same incident energies in both cases showing the equivalence between $\langle p_x/A \rangle$ and $\langle p_x^{dir} \rangle$ as far as balance energy is concerned. The latter quantity is more useful since it is stable than former one. These findings are in agreement with refs. [28, 29].

It has been advocated by several authors that the study of disappearance of flow can shed light on the magnitude of nn cross-section [3, 5, 8, 10, 12, 13, 16, 22, 24, 25, 26, 28, 29, 30, 31]. To check this point with reference to mass dependence, we show in fig. 3, the final stage $\langle p_x^{dir} \rangle$ as a function of the incident energy. The left panel is for $^{20}\text{Ne}+^{27}\text{Al}$, $^{64}\text{Zn}+^{58}\text{Ni}$ and $^{139}\text{La}+^{139}\text{La}$, respectively, for top, middle and bottom whereas top, middle and bottom of right hand side displays the results, respectively, of $^{40}\text{Ar}+^{45}\text{Sc}$, $^{93}\text{Nb}+^{93}\text{Nb}$ and $^{197}\text{Au}+^{197}\text{Au}$. The experimental data are displayed by stars whereas the present results with $\sigma=55$, 40 and 20 mb are shown, respectively, by solid circles, open squares and solid triangles. The $\langle p_x^{dir} \rangle$ obtained with energy dependent cross-section due to Cugnon (labeled as Cug) and the one that takes the medium into account (i.e. the G-matrix) are marked by solid diamonds and inverted triangles, respectively. First of all, we see that the medium effects in nn cross-section do not play any role at these low incident energies. The results obtained with Cugnon energy dependent cross-section and G-matrix medium dependent cross-section are roughly the same for heavier colliding nuclei where reactions are simulated at low incident energies. Some visible differences, however, can be seen in the case of light colliding nuclei where incident energy is relatively high. One also sees a linear enhancement in the nuclear flow with increase in the incident energy. Further, the role of different cross-sections is consistent through out the present mass range. The largest cross-section gives more positive flow which is followed by the second larger cross-section. Interestingly, these effects depend on the mass of the system. If one looks at the reaction of $^{20}\text{Ne}+^{27}\text{Al}$, one sees that the E_{bal} increases from 89 MeV/nucleon to 244 MeV/nucleon when nn cross-sections is reduced from 55 mb to 20 mb. Whereas the range of E_{bal} for the same cross-sections was 47-83 MeV/nucleon for $^{93}\text{Nb}+^{93}\text{Nb}$ reaction. If one goes to still heavier nuclei, $^{197}\text{Au}+^{197}\text{Au}$, the range of E_{bal} narrows down to 38-59 MeV/nucleon. In other words, a reduction in the cross-section by 64%

percent yields a change of 155 MeV/nucleon in the case of $^{20}\text{Ne}+^{27}\text{Al}$ reaction, whereas it is only 21 MeV/nucleon for the case of $^{197}\text{Au}+^{197}\text{Au}$. Similarly looking at the curves of $\sigma=55$ and 40 mb, a reduction in the cross-section by 27% yields a difference of 30 MeV/nucleon in the E_{bal} for $^{20}\text{Ne}+^{27}\text{Al}$ reaction whereas nearly 4 MeV difference exists for the case of $^{197}\text{Au}+^{197}\text{Au}$ reaction. This result, which is in agreement with the findings of refs. [12, 13], depicts that for heavier colliding nuclei, the E_{bal} is independent of the cross-section one is choosing. Further, the standard energy dependent nn cross-section (Cug) fails to reproduce the observed balance energy in almost all the cases. However, a constant cross-section of 40 mb strength seems to be closer to the experimental observed balance energy. This conclusion is supported by several other groups where a cross-section of 30-40 mb was used to reproduce the experimental data [8, 10, 22, 24, 25, 26, 29, 30, 31, 35, 36]. This will be discussed in detail in the following paragraphs.

It has been argued in refs. [28, 37] that the flow at any point during the reaction can be divided into the parts emerging from the (attractive) mean field potential and (repulsive) nn collisions. Following [28], we decomposed the transverse momentum into the contributions created by the mean field and two-body nn collisions. This extraction, which is made from the simulations of the QMD model, is done as following [28]: Here at each time step during the collision, momentum transformed by the mean field and two-body collision is analyzed separately. Naturally, we get two values at each step which can be followed throughout the reaction. The total transverse momentum can be obtained by adding both these contributions.

In fig. 4, we display the final state $\langle p_x^{dir} \rangle$ decomposed into two parts i.e. into the mean field and two-body collision parts as a function of the incident energies for different colliding systems as reported in fig. 3. Again a linear enhancement in the flow with energy can be seen. Further, the contribution of the mean field remains attractive throughout the energy range whereas collision contribution is always repulsive. The balancing of both these contributions results in net zero flow. One should, however, keep in the mind that the contribution of the mean field potential may even turn repulsive at higher incident energies [37].

In fig. 5, we display the energy of vanishing flow (E_{bal}) as a function of the combined mass of the system for fifteen different colliding pairs that range from $^{20}\text{Ne}+^{27}\text{Al}$ to $^{197}\text{Au}+^{197}\text{Au}$. In our earlier communication [31], a prediction of E_{bal} for $^{238}\text{U}+^{238}\text{U}$ was also reported. It is worth mentioning that this is the first ever attempt that deals with as many as fifteen systems. Earlier attempts of mass dependence [5, 12, 16, 17, 26] had taken about six cases into account. Apart from the experimental data, we also show our results for $\sigma=35$ and 40 mb. All curves are a fit of the form $c.A^\tau$ using χ^2 minimization procedure. The experimental data can be fitted by $\tau_{expt} = -0.42079 \pm 0.04594$ whereas our present results

with $\sigma=40$ mb has $\tau_{40} = -0.41540 \pm 0.08166$. The results with $\sigma=35$ mb yields $\tau_{35} = -0.43037 \pm 0.08558$. Exclusively, one can extract the following:

- The present value of τ_{expt} differs from the earlier reported results ($\tau_{expt} = -1/3$ for $A \leq 200$ [5] and $\tau_{expt} = -0.46 \pm 0.06$ [16] for $A \leq 400$ mass). Note that in earlier attempts [12, 16], the data of NSCL alone was used to fit the power law. In the present case, we have taken data from different sources amounting to 15 reactions. Therefore, the present analysis is universal in nature.
- The present theoretical value $\tau_{40} = -0.41540 \pm 0.08166$ is the closest one obtained so far. In earlier reports [5], the τ_{expt} was $-1/3$ whereas BUU model yielded $-0.28 \leq \tau_{th} \leq -0.32$. In another study [16], the τ_{expt} was -0.46 ± 0.06 whereas BUU model has $\tau_{th} = -0.41 \pm 0.03$. In other words, the present QMD model with a stiff EOS along with $\sigma=35$ -40 mb can explain the data much better than any other theoretical calculations. Our present analysis has much wider mass spectrum than any early attempt. Some deviations in the middle order are also reported by other authors [25]. The $\sigma=40$ explains E_{bal} in heavier nuclei whereas $\sigma=35$ reproduces a middle order nicely.
- From the figure, it is also evident that a true cross-section for this energy domain should be between 35 and 40 mb. This conclusion is very important since a wide range of masses was used for the present analysis. Our conclusion about the strength of the nn cross-section is in agreement with large number of earlier calculations on disappearance of flow and other phenomena in heavy-ion collisions [8, 10, 22, 24, 25, 26, 29, 30, 31, 35, 36]. As noted in ref. [26], this value of nn cross-section is still much less than the actual averaged free nn cross-section which is about 60 mb [38]. In the case of fragmentation, a larger cross-section of $\sigma=55$ mb is also suggested [35].

We have also tried to fit the balance energy in terms of other parameters such as the charge of the colliding nuclei. This attempt is shown in fig. 6 where E_{bal} is plotted as a function of the total atomic number of the system. In the upper part, we display the full range of the systems whereas in the lower part, only heavier nuclei are taken into picture. A power law $\propto Z^\tau$ fits the data nicely. Now τ is -0.46703 ± 0.04745 (-0.45808 ± 0.08688) for experimental data (theoretical results) which is larger compared to mass power law ($\tau = -0.42079 \pm 0.04594$ (-0.41540 ± 0.08166)) for experiment data (theoretical results). This difference in the slopes stems from the different charge/mass ratio in lighter and heavy nuclei. Interestingly, the value of τ for heavier nuclei (see fig. 6(b)) is -0.59316 ± 0.0622 (-0.58483 ± 0.11409). This result, which is in agreement

with ref. [16], shows the dominance of the Coulomb interactions in heavier colliding nuclei. It would be of further interest to investigate whether the flow due to the collision and mean field parts (at the balance energy) exhibit any mass dependence or not. We display, in fig. 7, the flow $\langle p_x^{dir} \rangle$ at balance energy due to the collision (upper) and mean field parts (lower). Interestingly, we do not see any clear mass dependence. Rather very weak dependence (with $\tau = -0.09427 \pm 0.08379$) exists on the system size. This is in agreement with ref. [37], where a similar conclusion was drawn.

IV. SUMMARY

We have studied the mass dependence of the disappearance of flow in large number of colliding nuclei using QMD model. As many as fifteen reactions with masses between 47 and 476 were studied for the first time, where experimental balance energy was available. Our findings suggest a weak dependence of different cross-sections for heavier colliding nuclei in agreement with [12]. For the first time, fifteen different reactions were studied and our calculations with a stiff equation of state are in excellent agreement with experimental data. We could reproduce the slope of the power law ($\propto A^\tau$) very well. Our calculations suggest a cross-section of 35-40 mb in this incident energy domain. We also showed that the collective flow due to mean field is attractive whereas it is repulsive for collision part. The balancing of these two parts results in the disappearance of flow.

This work is supported by the grant (No. SP/S2/K-21/96) from Department of Science and Technology, Government of India.

-
- [1] W. Scheid, H. Müller, and W. Greiner, Phys. Rev. Lett. **32**, 741 (1974).
- [2] B.A. Li and A.T. Sustich, Phys. Rev. Lett. **82**, 5004 (1999).
- [3] Y.M. Zheng, C.M. Ko, B.A. Li, and B. Zhang, Phys. Rev. Lett. **83**, 2534 (1999).
- [4] J.J. Molitoris and H. Stöcker, Phys. Lett. B **162**, 47 (1985); V. de la Mota, F. Sebillie, M. Farine, B. Remaud, and P. Schuck, Phys. Rev. C **46**, 677 (1992); G.F. Bertsch, W.G. Lynch, and M.B. Tsang, Phys. Lett. B **189**, 384 (1987); D. Krofcheck *et al.*, Phys. Rev. Lett. **63**, 2028 (1989).
- [5] G.D. Westfall *et al.*, Phys. Rev. Lett. **71**, 1986 (1993).
- [6] R. Pak, O. Bjarki, S.A. Hannuschke, R.A. Lacey, J. Lauret, W.J. Llope, A. Nadasen, N.T.B. Stone, A.M. Vander Molen, and G.D. Westfall, Phys. Rev. C **54**, 2457 (1996); R. Pak *et al.*, *ibid.* **53**, R1469 (1996).
- [7] J.C. Angelique *et al.*, Nucl. Phys. **A614**, 261 (1997).
- [8] J.P. Sullivan *et al.*, Phys. Lett. B **249**, 8 (1990).
- [9] D. Krofcheck *et al.*, Phys. Rev. C **43**, 350 (1991); C.A. Ogilvie *et al.*, Phys. Rev. C **42**, R10 (1990).
- [10] Z.Y. He *et al.*, Nucl. Phys. **A598**, 248 (1996).
- [11] D. Cussol *et al.*, Phys. Rev. C **65**, 044604 (2002).
- [12] D.J. Magestro, W. Bauer, and G.D. Westfall, Phys. Rev. C **62**, 041603(R) (2000).
- [13] G.D. Westfall, Nucl. Phys. **A681**, 343c (2001); R. Pak *et al.*, Phys. Rev. Lett. **78**, 1026 (1997); R. Pak *et al.*, *ibid.* **78**, 1022 (1997).
- [14] D. Krofcheck *et al.*, Phys. Rev. C **46**, 1416 (1992).
- [15] W.M. Zhang *et al.*, Phys. Rev. C **42**, R491 (1990); M.D. Partlan *et al.*, Phys. Rev. Lett. **75**, 2100 (1995); P. Crochet *et al.*, Nucl. Phys. **A624**, 755 (1997).
- [16] D.J. Magestro, W. Bauer, O. Bjarki, J.D. Crispin, M.L. Miller, M.B. Tonjes, A.M. Vander Molen, G.D. Westfall, R. Pak, and E. Norbeck, Phys. Rev. C **61**, 021602(R) (2000).
- [17] A. Buta *et al.*, Nucl. Phys. **A584**, 397 (1995).
- [18] J. Singh, S. Kumar, and R.K. Puri, Phys. Rev. C **62**, 044617 (2000).
- [19] R.K. Puri and S. Kumar, Phys. Rev. C **57**, 2744 (1998); Zhuxia Li, C. Hartnack, H. Stöcker, and W. Greiner, *ibid.* **44**, 824 (1991).
- [20] C. Liewen, Z. Fengshou, and J. Genming, Phys. Rev. C **58**, 2283 (1998).
- [21] B.A. Li, Z. Ren, C.M. Ko, and S.J. Yennello, Phys. Rev. Lett. **76**, 4492 (1996).
- [22] H. Zhou, Z. Li, Y. Zhuo, and G. Mao, Nucl. Phys. **A580**, 627 (1994).
- [23] D. Klakow, G. Welke, and W. Bauer, Phys. Rev. C **48**, 1982 (1993).
- [24] H.M. Xu, Phys. Rev. C **46**, R389 (1992); H.M. Xu, Phys. Rev. Lett. **67**, 2769 (1991).
- [25] B.A. Li, Phys. Rev. C **48**, 2415 (1993).
- [26] H. Zhou, Z. Li, and Y. Zhuo, Phys. Rev. C **50**, R2664 (1994).
- [27] S. Soff, S.A. Bass, C. Hartnack, H. Stöcker, and W. Greiner, Phys. Rev. C **51**, 3320 (1995).
- [28] E. Lehmann, A. Faessler, J. Zipprich, R.K. Puri, and S.W. Huang, Z. Phys. A **355**, 55 (1996).
- [29] S. Kumar, M.K. Sharma, R.K. Puri, K.P. Singh, and I.M. Govil, Phys. Rev. C **58**, 3494 (1998).
- [30] A. Sood and R.K. Puri, Symposium on Nuclear Physics, **45B**, 288 (2002); A. Sood and R.K. Puri, VIII Int. Conf. on Nucleus-Nucleus Collisions, Moscow, Russia, June 17-21 (2003)- accepted.
- [31] A.D. Sood, R.K. Puri, and J. Aichelin, Phys. Rev. Lett., (2003)- submitted.
- [32] S. Kumar, R.K. Puri, and J. Aichelin, Phys. Rev. C **58**, 1618 (1998).
- [33] J. Aichelin, Phys. Rep. **202**, 233 (1991); J. Aichelin and H. Stöcker, Phys. Lett. B **176**, 14 (1986).
- [34] C. Hartnack, R.K. Puri, J. Aichelin, J. Konopka, S.A. Bass, H. Stöcker, and W. Greiner, Eur. Phys. J A **1**, 151 (1998).
- [35] H.W. Barz, J.P. Bondorf, D. Idier, and I.N. Mishustin, Phys. Lett. B **382**, 343 (1996).
- [36] C. Roy *et al.*, Z. Phys. A **358**, 73 (1997).
- [37] B. Blättel, V. Koch, A. Lang, K. Weber, W. Cassing, and U. Mosel, Phys. Rev. C **43**, 2728 (1991).
- [38] K. Chen, Z. Fraenkel, G. Friedlander, J.R. Grover, J.M. Miller, and Y. Shimamoto, Phys. Rev. **166**, 949 (1968).

Figure Captions

FIG. 1. The averaged $\langle p_x/A \rangle$ as a function of $Y_{c.m.}/Y_{beam}$. Here we display the results at different incident energies using a stiff equation of state along with $\sigma=40$ mb. The reactions of $^{20}\text{Ne}+^{20}\text{Al}$ and $^{40}\text{Ar}+^{45}\text{Sc}$ are at 150 fm/c whereas those of $^{64}\text{Zn}+^{58}\text{Ni}$, $^{93}\text{Nb}+^{93}\text{Nb}$, $^{139}\text{La}+^{139}\text{La}$ and $^{197}\text{Au}+^{197}\text{Au}$ are at 300 fm/c.

FIG. 2. The time evolution of $\langle p_x^{dir} \rangle$ as a function of time. Here again results are for stiff equation of state along with $\sigma=40$ mb.

FIG. 3. The $\langle p_x^{dir} \rangle$ as a function of the incident energy. The results for different cross-sections of 55, 40 and GMC are represented, respectively, by the solid circles, open squares and solid inverted triangles whereas for Cug and 20 mb are represented by solid diamonds and solid triangles. A stiff equation of state has been used. All lines are to guide the eyes.

FIG. 4. The decomposition of $\langle p_x^{dir} \rangle$ into collision and mean field parts as a function of incident beam

energy. Here results are displayed for $\sigma=40$ mb. Stars are the experimental balance energy.

FIG. 5. The balance energy as a function of combined mass of the system. The experimental points along with error bars are displayed by solid stars whereas our theoretical calculations for $\sigma=35$ and 40 mb are shown by open triangles and squares. The lines are the power law $\propto c.A^\tau$. The solid, dashed and dash-dotted lines represent the power law fit for experimental points, with $\sigma=40$ and 35 mb, respectively.

FIG. 6. (a) Balance energy as a function of atomic number Z . Here we display the experimental results along with our calculations for $\sigma=40$ mb. The fits are obtained with χ^2 minimization for power law function $c.Z^\tau$. (b) Same as (a), but for heavier nuclei.

FIG. 7. The decomposition of the $\langle p_x^{dir} \rangle$ at balance energy into collision and mean field parts. The results are obtained using a stiff equation of state along with $\sigma=40$ mb.

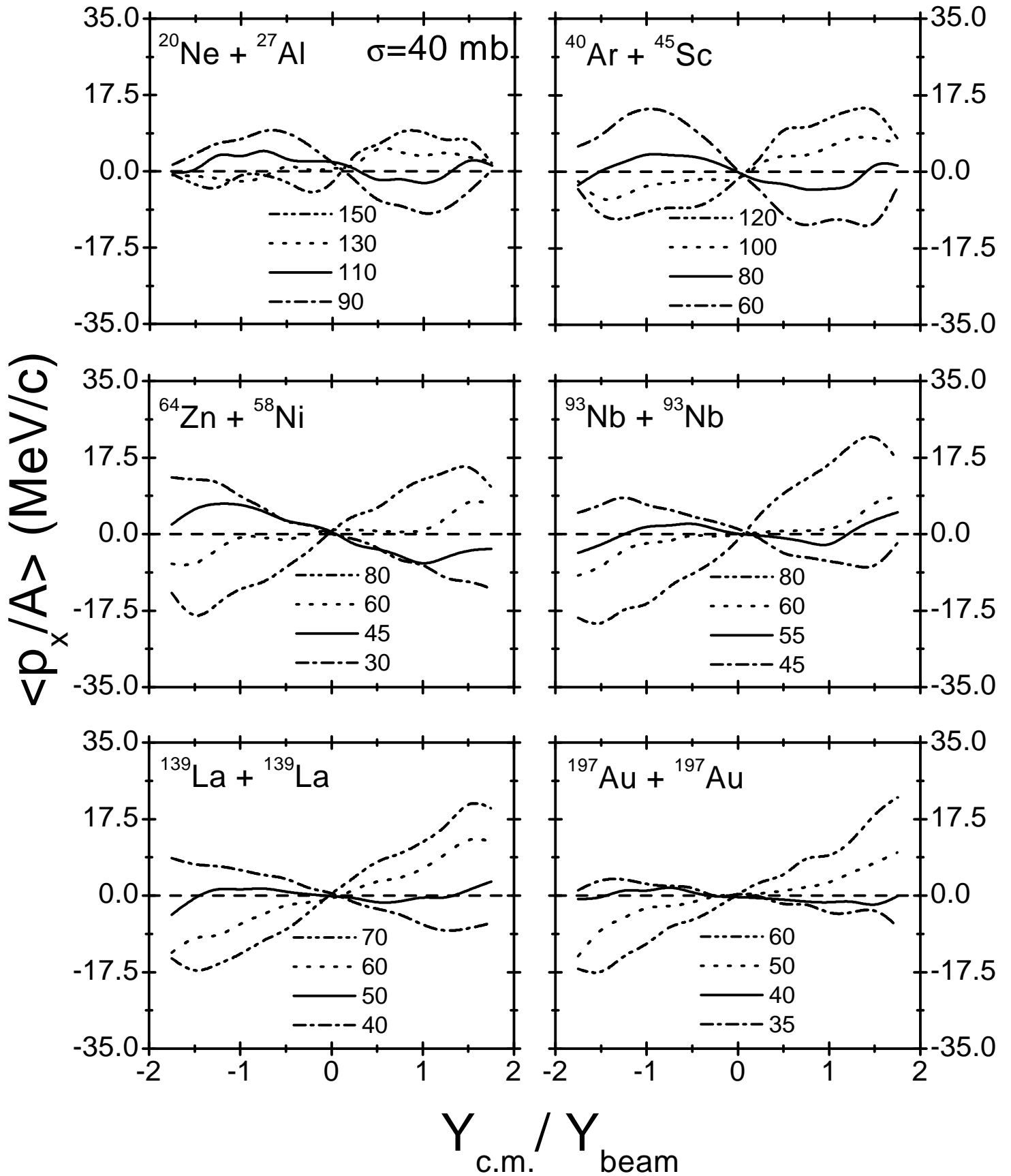


Fig. 1 "Mass Dependence of Disappearance" by Sood and Puri

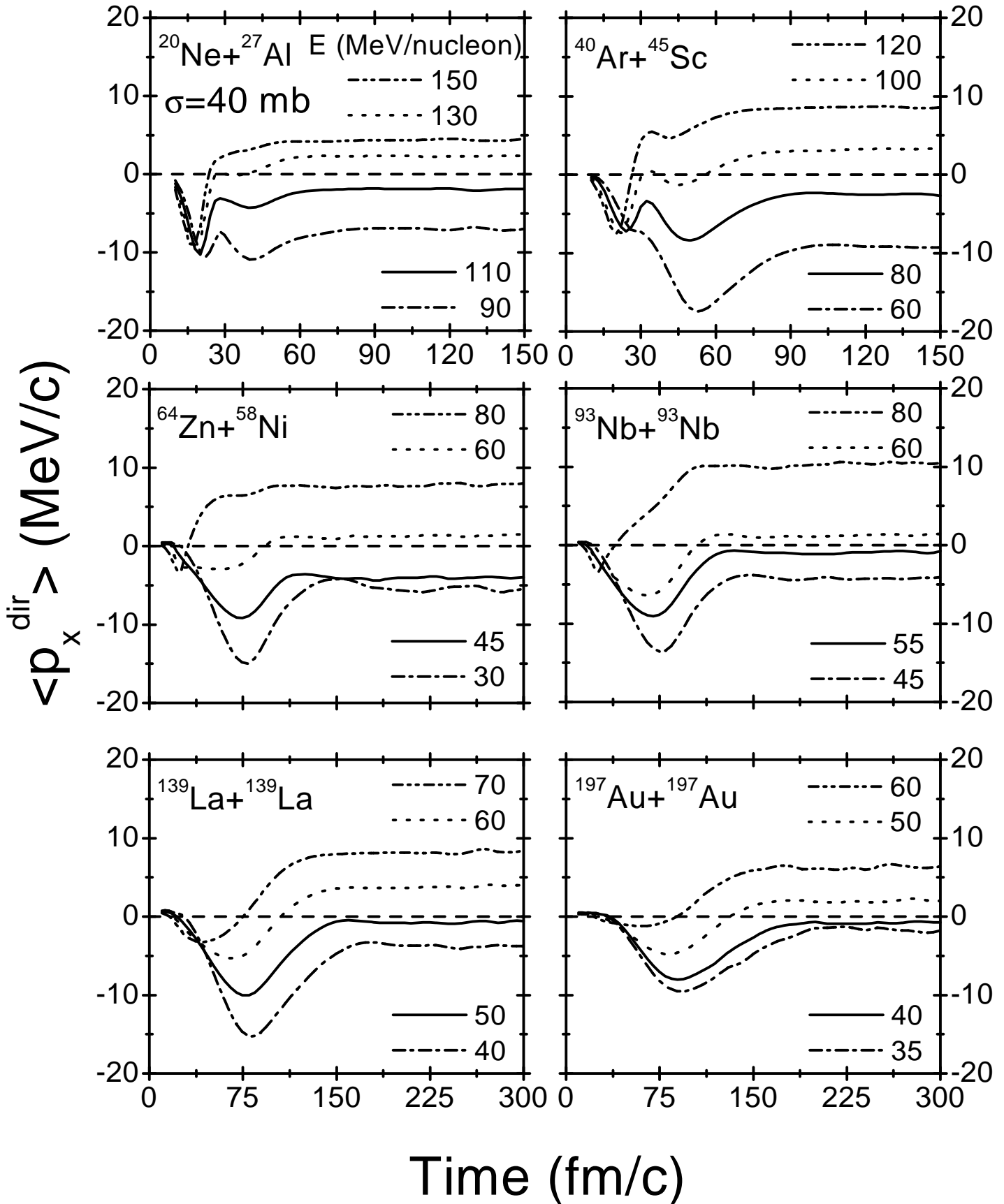


Fig. 2 "Mass Dependence of Disappearance" by Sood and Puri

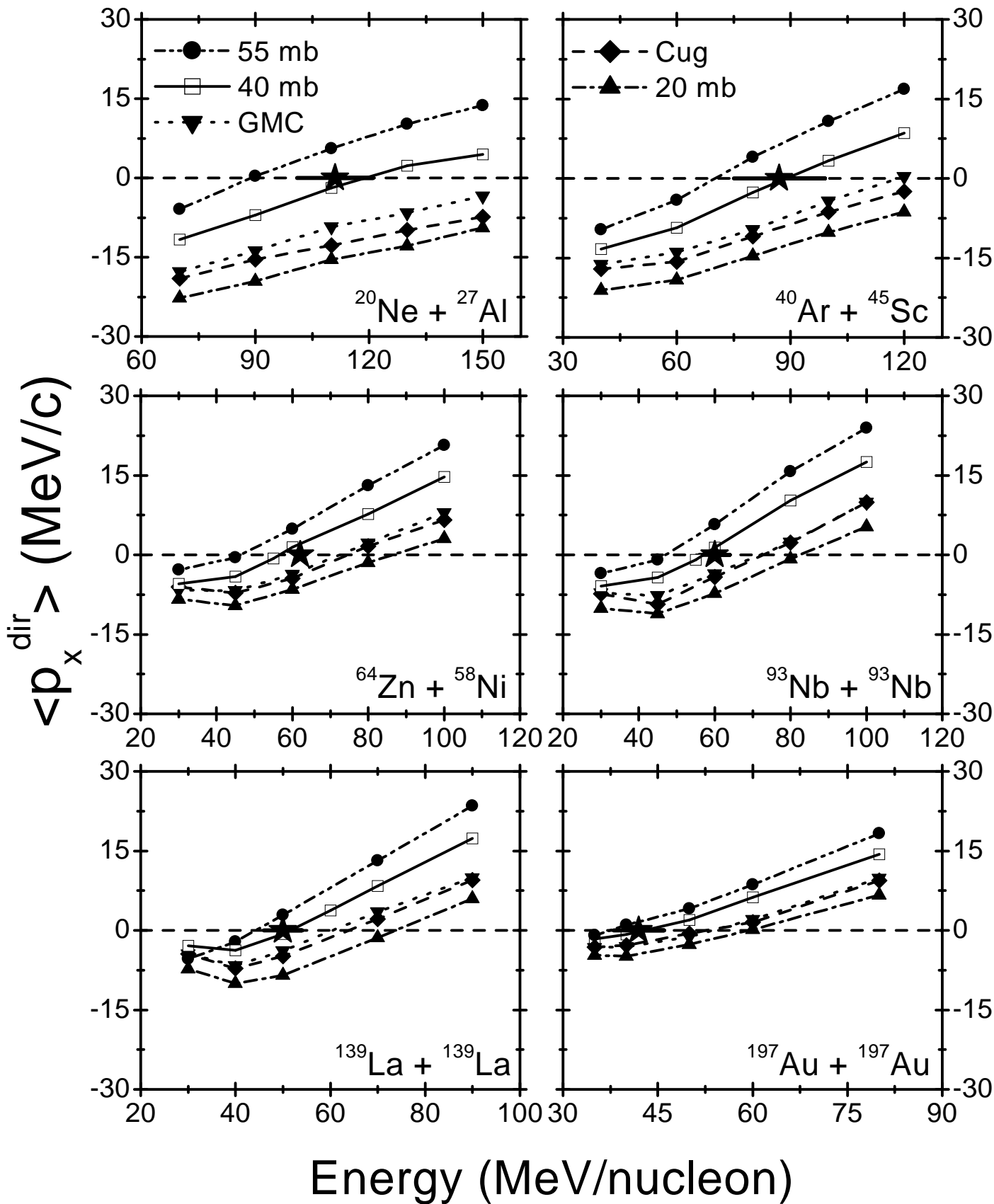


Fig. 3 "Mass Dependence of Disappearance" by Sood and Puri

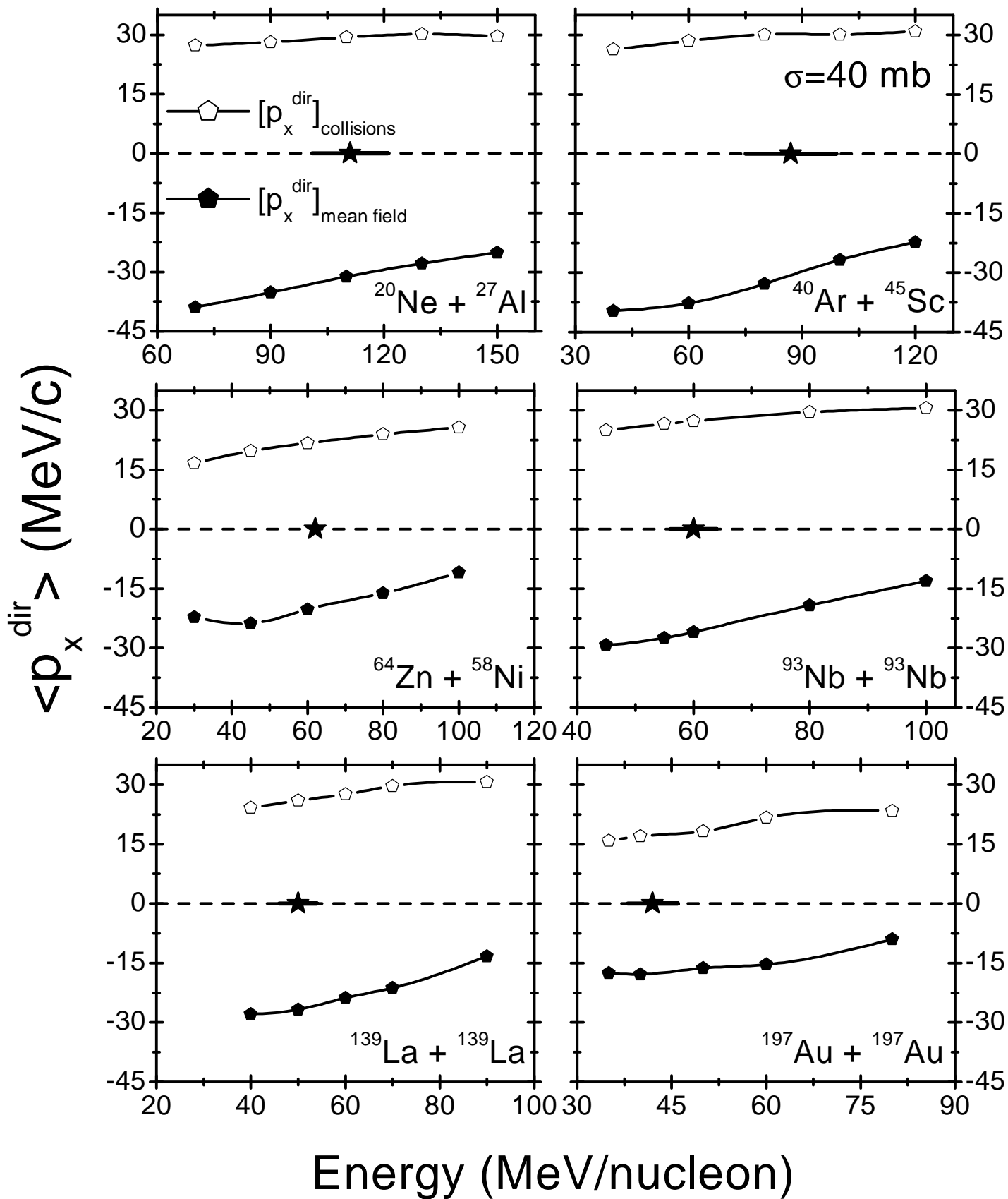


Fig. 4 "Mass Dependence of Disappearance" by Sood and Puri

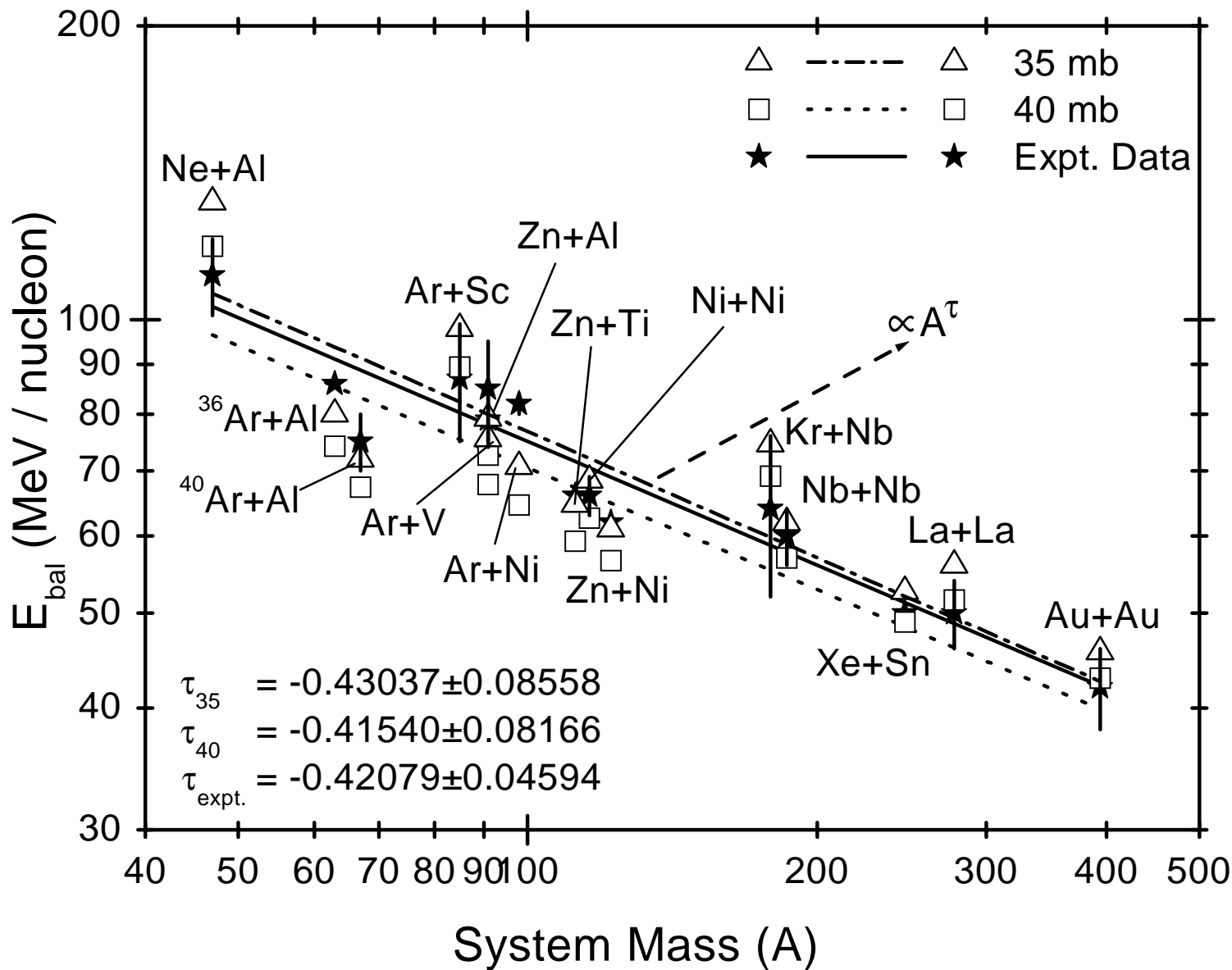


Fig. 5 "Mass Dependence of Disappearance" by Sood and Puri

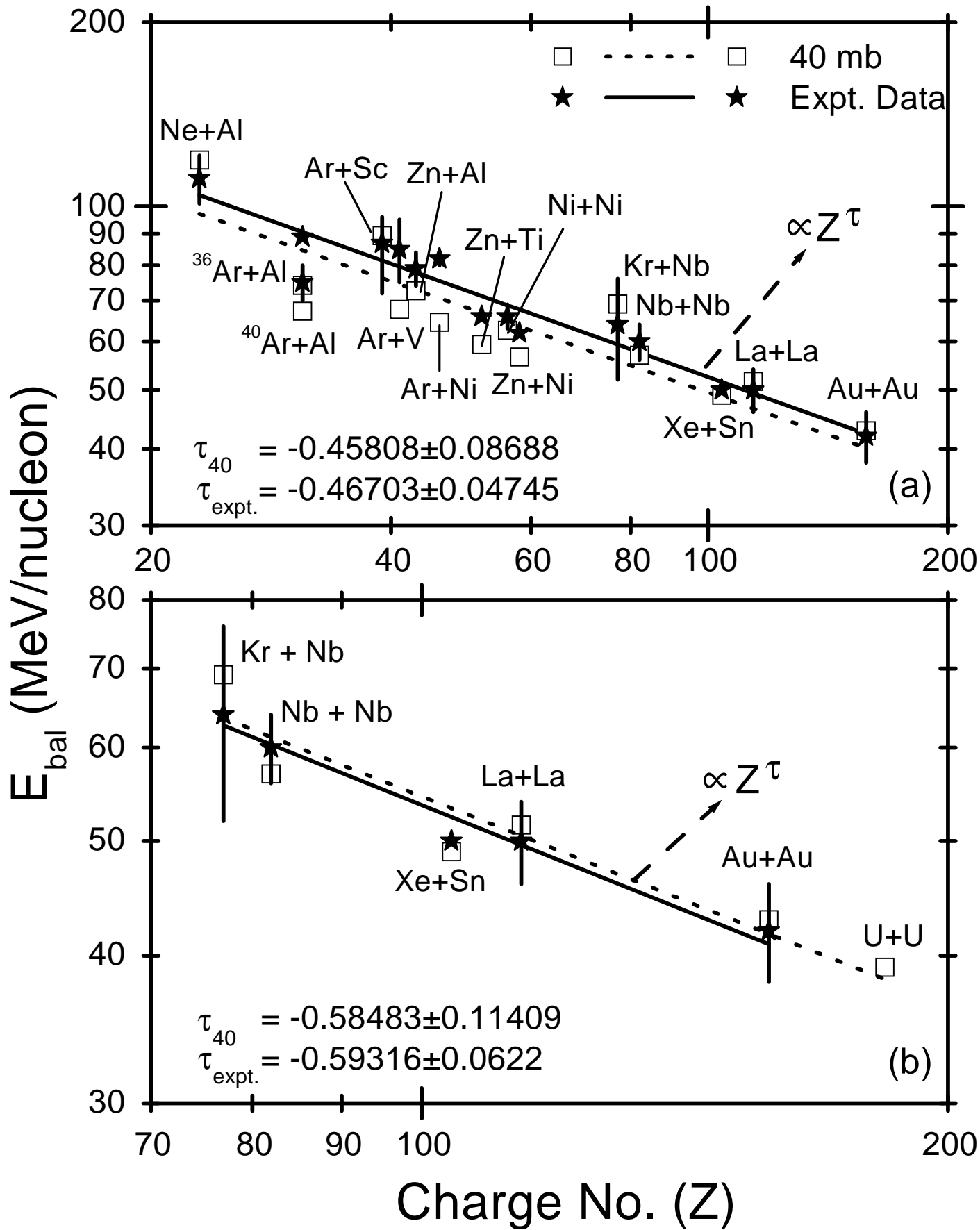


Fig. 6 "Mass Dependence of Disappearance" by Sood and Puri

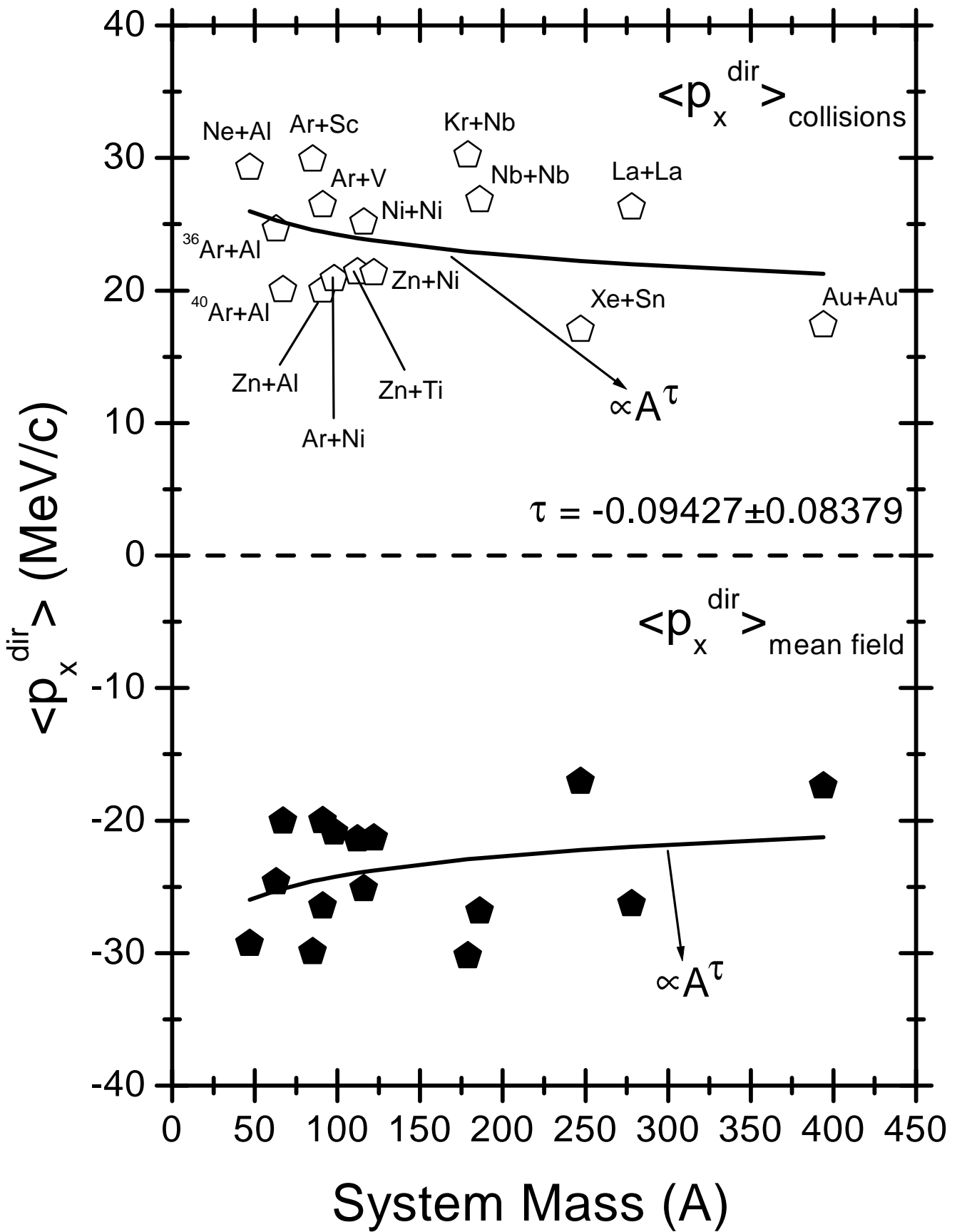


Fig. 7 "Mass Dependence of Disappearance" by Sood and Puri